European Journal of Clinical Pharmacy

Print ISSN: 2385-409X **Online ISSN**: 3105-0409

Website: https://farmclin.com/

Original Research Article

A Compact Orthogonal CPW-Fed MIMO Antenna for Sub-6 GHz 5G Applications

Article History:

Name of Author:
G. Mohan[1] , M. Pranay Kumar[2]

Affiliation: *[1](Ph.D Scholar, Dept. of ECE, Chaitnya Deemed to be University, Telangana, India)*
[2](Assoc. Professor, Dept. of ECE, Chaitnya Deemed to be University, Telangana, India)

***Received**:* 10-11-2025
***Revised**:* 26-11-2025
***Accepted**:* 09-12-2025
***Published**:* 31-12-2025

Abstract: ***Background***: A compact MIMO antenna with circularly polarized is presented along with a CPW feed and a simple decoupling structure using Ansys HFSS software. The MIMO antenna operates in a frequency range of 3.3-3.8GHz, which is placed on FR4 epoxy substrate making it acceptable for 5G applications. Designed antenna covers all of the major frequency bands in the 5G range (3.3-3.69 GHz). The suggested final orthogonal antenna's total dimensions are 89.5×34×0.8 mm3. The design typically involves Coplanar Waveguide (CPW) feeding structure which is suitable for achieving wide operating bandwidth and good impedance matching. To achieve the desired reflection coefficient of less than -10 dB, precise tuning of the antenna's geometry and feed network are incorporated. Slots are added to the basic antenna patch. A good axial ratio of 3dB bandwidth exists in the range of 3.3-3.9 GHz. A dielectric constant of 4.4 and a loss tangent of 0.02 in order to simulating and analyzing the parameters. The simulated design's MIMO diversity parameters have been obtained and compared with standard requirements. The designed enhanced bandwidth circularly polarized CPW-Fed MIMO antenna suitable for a variety of 5G applications.

Keywords: Circular polarization; copalnar wave guide MIMO antenna; channel capacity loss (CCL); Sub-6 GHz 5G

INTRODUCTION

The technology can significantly enhance the data transfer capacity for wireless connections. This results in faster speeds, improved performance, and more effective utilization of the available spectrum [1]-[5]. The integration of Coplanar Waveguide (CPW) feeding and circular polarization (CP) in antenna design for 5G applications offers several advantages. CPW-fed antennas provide wideband performance, making them suitable for 5G-enabled devices like smartphones, IoT devices, and smart wearables. They are compact and low-profile, allowing for efficient power transfer [6]-[10]. Circularly polarized antennas offer enhanced polarization diversity, overcoming signal fading and polarization mismatches in 5G MIMO systems. They also exhibit low cross-polarization, minimizing interference and improving system performance. In 5G networks, circular polarization contributes to stronger communication links by reducing multipath propagation. This combination of CPW feeding and Circular polarization in antenna design enables reliable solution [10]-[15]. The demand for fast, low-latency wireless communication networks is growing, leading to the development of 5G applications. Innovative antenna technologies are needed for 5G networks in order to provide extremely fast data transfer, high levels of connectivity, and smooth interaction with a wide range of devices and applications. In order to cover all major frequency bands of WiMAX (3.4–3.69GHz) and 5G (3.3–3.69GHz), applications. By leveraging MIMO technology, antennas in 5G applications can support multiple streams of data, improving overall network capacity and reliability. As a result, researching MIMO systems is crucial to creating 5G communication systems [16]-[20]. Decoupling is a crucial aspect of MIMO antenna design, ensuring each element operates independently and efficiently without interference. It helps minimize mutual coupling, reduces correlation, enhances diversity and capacity, maintains the desired radiation pattern, and reduces interference from external sources. The effectiveness of wireless communication systems is intricately tied to various factors that influence signal propagation, transmission efficiency, and reception quality [21]-[25]. MIMO Diversity Parameters are key elements in wireless communication systems. ECC gauges the correlation between two antennas, CCL quantifies the data rate reduction caused by factors such as interference. TARC assesses the power reflected by an antenna, MEG computes the average power transmitted in various directions, and DG focuses on the enhancement in signal quality from using multiple antennas [26]-[30]. These factors are essential for enhancing wireless network performance, efficiency, and ensuring reliable connectivity for users. In this paper, a broad bandwidth has been obtained with the incorporation of three microstrip lines and produced a circular polarization characteristic using an i-shaped microstrip line in the desired frequency band 3.3 GHz to 3.8 GHz.

II. DESIGN METHODOLOGY

A. Single Element Antenna Design

Fig.1 depicts the designed antenna structure in 3 stages. It was built using an FR4 substrate with a thickness of 0.8 mm. The substrate length, Ls, was 34 mm on each side, making the overall size 34 mm square. The antenna's feed was using a CPW- FED configuration. The T-shaped microstrip lines had geometric parameters Pl1, Wp1, Pl2, and Wp2. To achieve impedance matching, three microstrip lines with geometric parameters L1, Ws, and L2 were used. The i-shaped microstrip line, with parameters Li, Wi, and ri, was used for circular polarization.

Fig. 2 displays the structural outline of proposed single element antenna design. Table I shows the values of the dimensions. The lowest cut-off frequency will be referred as the dominant TE mode, and it is represented by the strip lines pl1 and pl2, which contribute to TE11 and TE12 correspondingly, by using the (1), the square slot dimensions are obtained.

RESULTS

$$c = \frac{C}{2\pi\sqrt{\varepsilon_{reff}}} \times \sqrt{\left[\left(\frac{m\pi}{a}\right)^2 + \left(\frac{n\pi}{b}\right)^2\right]} \qquad (1)$$

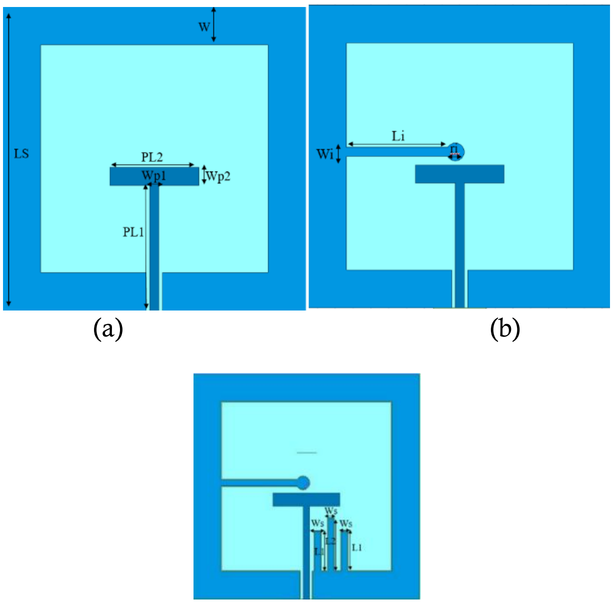

(a) (b)

(c)

Fig. 1. Three stages in the antenna design process (a) Stage 1 (b) Stage 2 (c) Stage 3 (Proposed)

TABLE I. DIMENSIONS OF THE PROPOSED SINGLE ELEMENT ANTENNA.

Parameter	Value(mm)	Parameter	Value(mm)
Ls	34	Wg	16.1
W	4.25	Li	12
H	0.8	Wi	1
Pl1	14	ri	1
Pl2	10	L2	8
Wp2	2	Ws	1

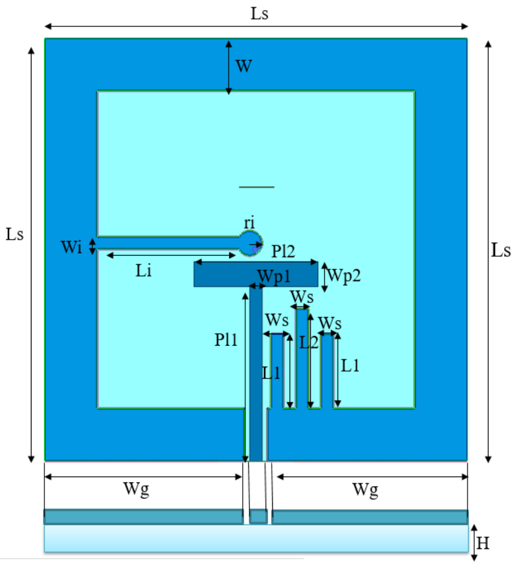

Fig. 2. Structure and dimensions of the single element antenna

Single Element Antenna Performance

It seems that the antenna underwent several stages of development to address certain issues encountered along the way. In the first stage, a CPW T- shape feed arrangement was utilized, which allowed for strong impedance matching and a wide bandwidth of 150 MHz from 3.97 to 4.12 GHz. However, an axial ratio issue was encountered, which led to the integration of an i-shaped microstrip line in Stage 2. This resulted in an improvement to the 3 dB axial ratio characteristics, although the impedance matching was not optimal. The antenna demonstrated a relatively wide bandwidth of 1360 MHz, spanning from 2.31 to 3.67 GHz. Moving on to Stage 3, the impedance was connected to three microstrip lines on the ground, leading to a favorable -10 dB reflection coefficient bandwidth of 1796 MHz from 2.941 to 4.737 GHz. It's worth noticing that the desired range of 3.3 to 3.8 GHz falls within this bandwidth, and the enhanced reflection coefficient at different stages is illustrated in the figure. By modifying the i-shaped strip's dimensional values, the axial ratio was calculated.

The best outcomes were achieved by testing multiple combinations of Li = 12, Wi = 1, and ri = 1. When compared to other dimension values, the achieved axial ratio at 215 MHz was less than 3 dB, as shown in *Fig. 4* in various stages. This is a good result. The gain curves are shown in *Fig. 5*, varied between 3.5 to 3.72dBi in the necessary range of 3.3 to 3.8GHz and all the parameters are listed in Table II.

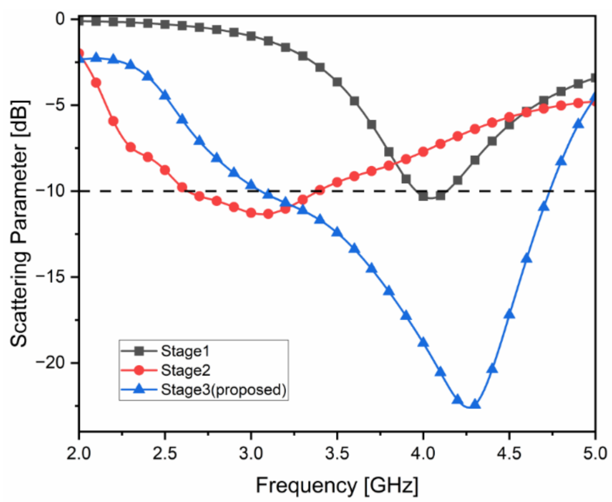

Fig. 3. Scattering parameters of Single Element antenna

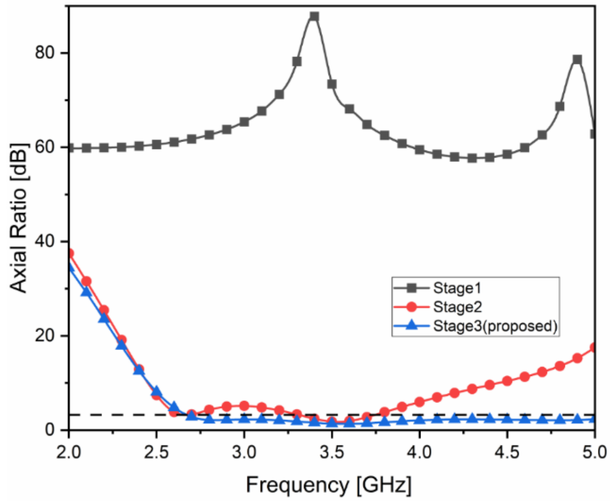

Fig. 4. Axial ratio of Single Element antenna

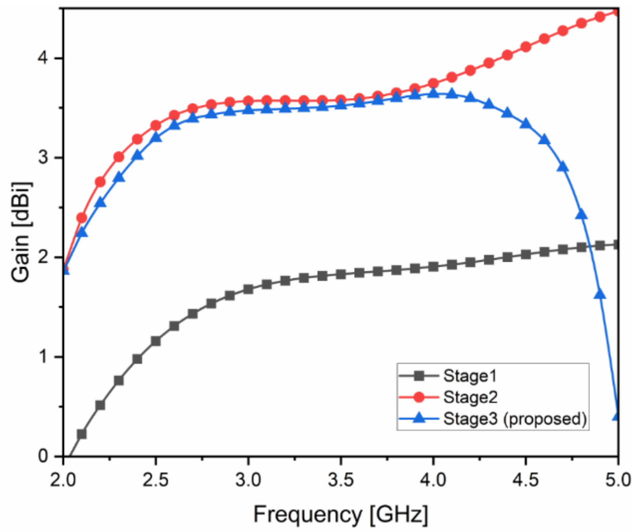

Fig. 5. Gain of Single Element antenna

TABLE II. RESULTS OF MONOPOLE ANTENNA IN THREE STAGES.

Antenna Stages	**Fc (MHz)**	**S11 ≤ -10dB BW(GHz) / % BW**	**3-dB A.R band width (GHz)**	**Peak gain (dBi)**
Stage 1	4.05	0.15/3.7	--	2.08
Stage 2	2.99	1.36/45.48	3.4-3.6	3.62
Stage 3	3.83	1.796/46.78	2.66-5	3.68

Desgin of the orthogonal MIMO antenna

The projected wideband MIMO antenna is a cost-effective solution. *Fig. 6* displays the antenna's design, which demonstrates how the radiating elements are intelligently positioned to improve mutual coupling via decoupling techniques. This not only ensures that the design is simple but also results in better performance. A shared ground plane supports the substrate. At the beginning, antenna elements were constructed through a mutual coupling of $S_{21} < -20$ dB. By integrating, it remained possible to observe low mutual interaction between the patches. Following several optimization steps, the most suitable antenna design was eventually achieved. Obtaining about 89.5 x 34 x 0.8 mm^3, the antenna takes up less volume than other designs. the planned two-element MIMO antenna has achieved a compact size by placing the two monopole antennas orthogonally and carefully positioning them with a distance of $\lambda/4$ = 21.5mm between them.

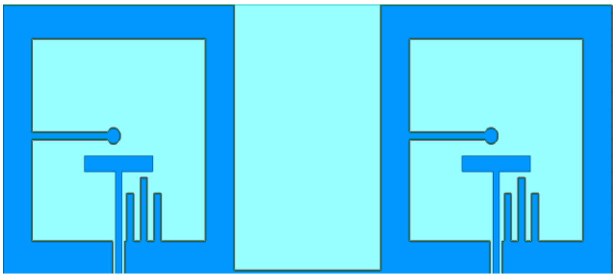

(a)

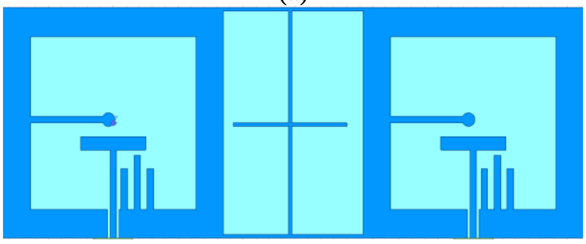

(b)

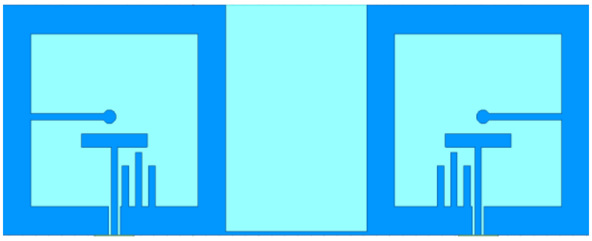

(c)

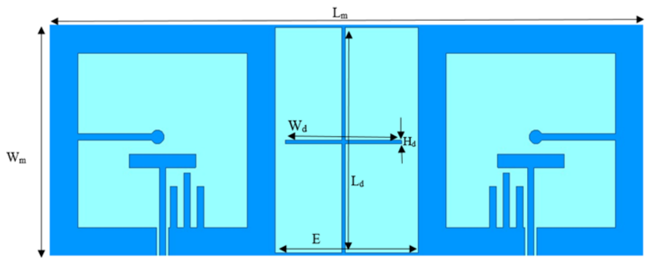

(d)

Fig. 6. Structure and dimensions of MIMO antennas (a) Side-by-Side without decoupling technique (b) Side-by-Side with decoupling technique (c) Proposed orthogonal without decoupling technique (d) Proposed orthogonal with decoupling technique

The orthogonal component is situated next to a shared ground plane to effectively minimize mutual coupling between the monopole elements in a MIMO antenna. The decoupling structure, represented by a "+" shaped structure placed between the monopole antennas, aims to reduce mutual coupling within the MIMO array. It seems that the MIMO antenna's dimensions have been altered by the addition of a "+" shaped decoupling structure. The measurements of the antenna are specified in millimeters, as per the parameters mentioned in Table III.

TABLE III. DIMENSIONS OF THE PROPOSED MIMO ANTENNA

Parameter	**Value (mm)**	**Parameter**	**Value (mm)**
L_m	89.5	L_d	34
W_m	34	W_d	12
E	21.5	H_d	1

MIMO Antenna Performance

The examination and discussion of performance parameters took place in this segment. Initially, the S-parameters, which include the reflection coefficient and transmission coefficient (isolation), of antenna are presented. The simulated results of the reflection coefficient for the designed MIMO antenna system can be seen in *Fig. 7*. The obtained S Parameters are S_{11} =1.3 GHz, S_{22} =1.2 GHz and S_{21} similar as S_{12} which is obtained -20dB below. S_{11} refers to the reflection coefficient of port one, and S_{21} refers to the transmission coefficient between port 1 and port 2. The proposed orthogonal element antenna configuration has a lower reflection coefficient than the side-by-side configuration at most frequencies. So, based on the comparison, the proposed Orthogonal element antenna configuration has better impedance matching compared to the side-by-side configuration. the reflection coefficient of S_{11} parameter shows below 30dB.

On coming to the S_{21} parameter, it is also good impedance matching at both, which means sufficient transmitting of the signal going into port. According to the context of the graph, S_{22} should be low across the desired frequency range, which means there should be minimal signal reflection at both ends to lead to efficient transmission. S_{21} parameter: the highest parameter indicates better isolation between two ports. From the graph, the proposed Orthogonal element configuration S_{21} has the highest value compared to the side-by-side configuration across most frequencies. Orthogonal element antenna maintains a consistently higher S_{21} value that is around 20 dB or lower compared to the side-by-side configuration that is around 25 dB or lower across most frequencies. generally, to be considered a 20 dB or lower S_{21} value for good isolation.

The bandwidth is 600 MHz from 3.3 to 3.9 GHz, and the resultant axial ratio is less than 3dB (*Fig 8*). In comparison to the side-by-side element, the suggested orthogonal element structure exhibits a better axial ratio. Based on the *Fig 9* the proposed orthogonal element configuration has the high gain after frequencies compared to the side-by-side element configuration increases steady as the frequency increases reaching a peak of around 4dBi at 3.5 GHz. It maintains the consistency compared to the side-by-side element configuration, so here the graph suggest that the proposed Orthogonal element configuration offers superior gain performance which leads to the stronger signal reception or transmission**.**

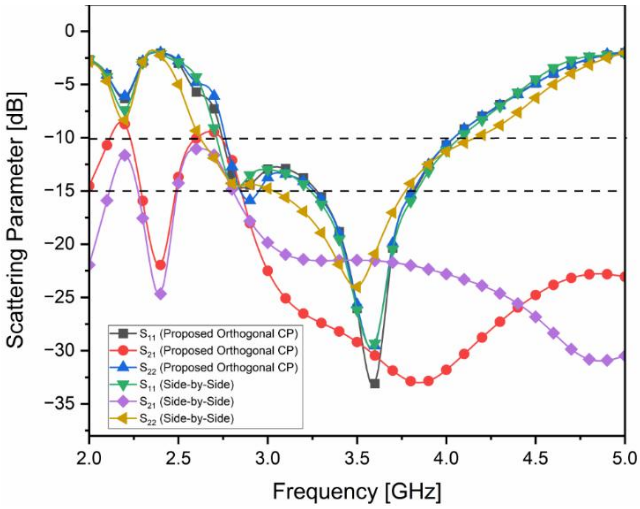

Fig. 7. Simulated Scattering parameters of Orthogonal MIMO antenna

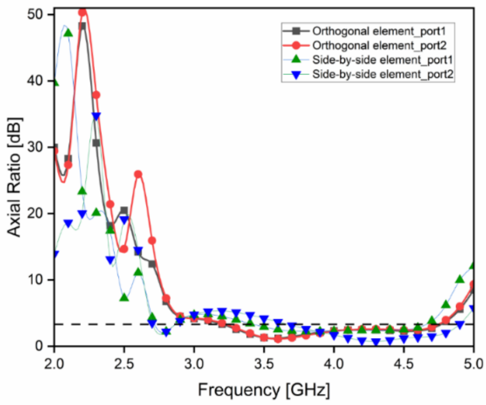

Fig. 8. Simulated Axial ratio of Orthogonal MIMO antenna

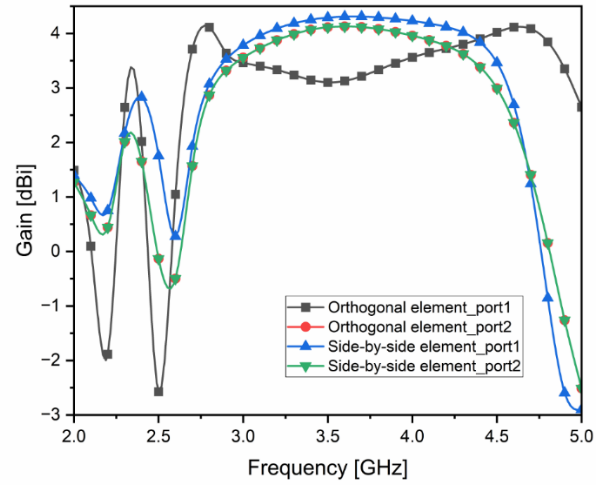

Fig. 9. Simulated Gain of Orthogonal MIMO antenna

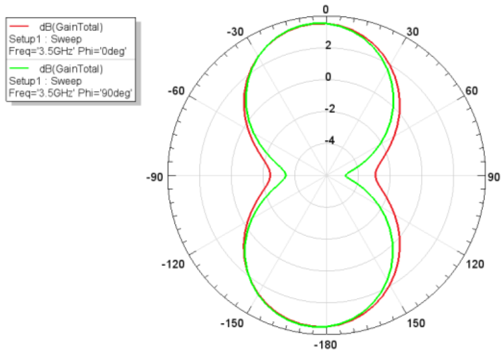

Fig. 10. Radiation plot for Single Element Antenna

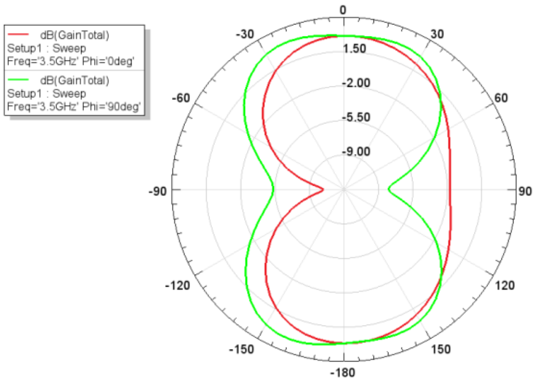

Fig. 11. Radiation plot for MIMOAntenna Port 1

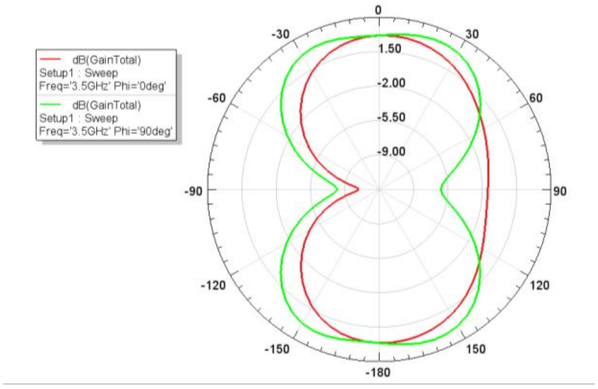

Fig. 12. Radiation plot for MIMOAntenna Port 2

MIMO Antenna evaluation parameters

Envelope correlation Coefficient (ECC):

ECC measures the correlation between different antennas in a wireless system. It helps assess how antennas interact with each other, affecting signal quality and overall system performance. The ECC can be determined by utilizing the following (2).

$$ECC = \rho_{nm} = \frac{|S_{nn}^{*}S_{nm}+S_{mn}^{*}S_{mm}|^2}{(1-(|S_{nn}|^2+|S_{mn}|^2))(1-(|S_{mm}|^2+|S_{nm}|^2))} \quad (2)$$

The maintenance of ECC values below 0.5 is crucial throughout the operational spectrum, indicating better isolation antennas. In *Fig. 13* The values are less than 0.02.

Diversity Gain (DG):

By exploiting diversity gain, wireless systems can combat fading, enhance signal robustness, and ensure uninterrupted communication. The DG has high values in the operational band, as *Fig. 13* displays. To measure direct measurement of the diversity gain from the ECC value is possible, and the outcome should be closer to 10dB. As a result, the DG value remains closer to 10dB throughout the entire operational band. The following (3) can be used for calculating the proposed MIMO antenna's diversity gain (DG).

$$DG=10 \times \sqrt{1-(ECC)^2} \quad (3)$$

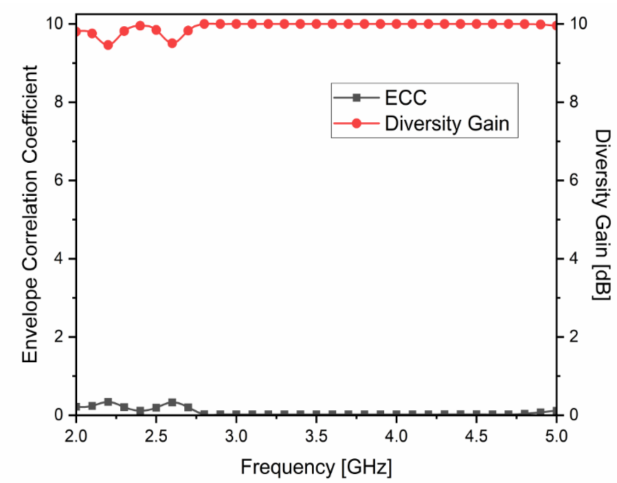

Fig. 13. ECC and Diversity Gain of the proposed MIMO design

Total Active Reflection Coefficient (TARC):

The Third major MIMO parameter is the TARC is a crucial measure that indicates the extent of power reflected back by antennas in a wireless. Its significance lies in minimizing signal losses, boosting signal strength, and enhancing overall network efficiency. Another key indicator demonstrating the interconnection between ports is the total active reflection coefficient (TARC). At a minimum value of 0, all incident power is emitted, while at a maximum value of 1, all incident power is mirrored, as *Fig. 14* displays. (4) is to find out the essential values.

$$\Gamma_a^t = \frac{\sqrt{\sum_{i=1}^{N} |b_r|^2}}{\sqrt{\sum_{i=1}^{N} |a_i|^2}} \quad (4)$$
$$[b] = [s][a]$$

The symbols ai and br stand for the incident and reflected signals, respectively. [S], [a], and [b] stand for the antenna's scattering matrix, excitation vector, and scattered vector, respectively.

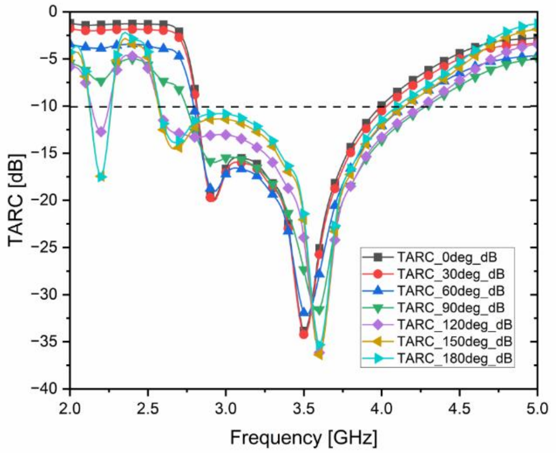

Fig. 14. TARC characteristics of the stated MIMO antenna.

Channel Capacity Loss:

CCL measures the reduction in capacity due to interference and signal degradation. Evaluating CCL allows wireless engineers to improve transmission techniques to mitigate capacity reductions. A CCL value of 0.5 bits/sec/Hz signifies excellent data transfer, while values above 0.5 bits/sec/Hz indicate inefficient data exchange. (5) is used to calculate CCL, as shown in *Fig. 15*. The CCL remains below 0.25 bits/sec/Hz across the operational band, indicating exceptional data transfer efficiency. This design demonstrates minimal data loss during transmission.

$$C(los) = -\log_2 \det(a)$$

$$a = \begin{bmatrix} \sigma_{ii} & \sigma_{ij} \\ \sigma_{ji} & \sigma_{jj} \end{bmatrix}$$
$$\sigma_{ii} = 1 - \left(|S_{ii}|^2 - S_{ij}^2\right) \quad (5)$$
$$\sigma_{ij} = -\left(S_{ii} * S_{ij} - S_{ji} * S_{ij}\right)$$

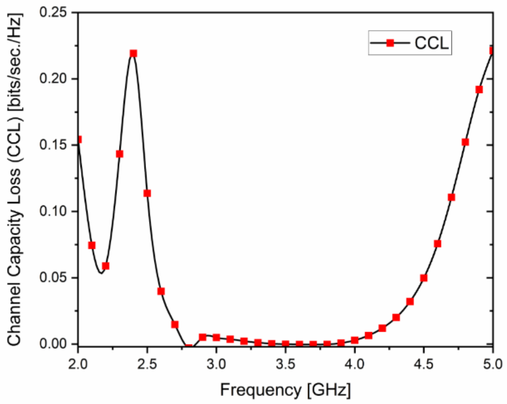

Fig. 15. CCL characteristics of the proposed MIMO design

Mean Effective Gain (MEG);

The mean effective gain (MEG), being the final parameter, illustrates the average increase in signal strength across all potential angles of an antenna. It is essential for the MEG to fall within the range of $-3 \leq$ MEG (dB) $< +3$ to ensure good diversity performance. The MEG values for MIMO antenna in the suggested design are shown in *Fig. 16*. As expected, the MEC values lie between the required range and the equation (6) is utilized to evaluate the MEG.

TABLE IV. EVALUATION OF THE PROJECTED WORK WITH EARLIER CPW-FED ANTENNAS

Ref. No.	Substrate /type	f_c (GHz)	S_{11}≤-10dB BW(GHz) /% BW	3-dBA.R band width	Peak gain (dBi)	Dimensions (mm^3)	Technique Used
[6]	FR- 4	3.7	0.6/16.21	340MHz (3.38-3.72) GHz	4	70 x 35 x16.1	Dual Polarization Technique
[9]	FR- 4	3.14	1.48/47.13	250MHz (3.4-3.65) GHz	6	80 x 50 x 15.6	Dual Polarization Technique
[14]	FR- 4	0.9	3.37/20.79	350MHz (3.22-3.57) GHz	5.07	40 x 40 x 19.6	Single Feeding Technique
[16]	FR- 4	3.68	0.04/1.08	40MHz (3.66-3.7) GHz	4.6	82 x 40 x 0.8	[illegible]
[20]	FR- 4	3.7	0.2/5.40	300MHz (3.55-3.85) GHz	5	12 5x 34 x 11.6	Diverse Technique of isolation
[22]	FR- 4	3.45	0.73/21.15	65MHz (3.15-3.80) GHz	4.83	95 x 49.7 x 1.6	Hybrid Technique
[25]	FR- 4	4.225	1.45/34.31	82MHz (3.58-4.40) GHz	6.5	35 x 35 x 1.6	Hybrid Technique
[29]	FR- 4	3.7	0.6/16.21	35MHz (3.45-3.8) GHz	3.8	70 x 35 x 14.5	Dual Polarization Technique
Proposed MIMO	FR- 4	3.39	3.39/38.32	600MHz (3.3-3.9) GHz	4	89.5 x 34 x 0.8	Decoupling Technique

$$MEG_i = 0.5\mu_{irad} = 0.5\left(1 - \sum_{j=1}^{K} |S_{ij}|\right) \qquad (6)$$

The symbol 'K' indicates the number of antennas, 'i' indicates the particular antenna under observation, and 'μ_{irad}' indicates the radiation efficiency. The comparison of presented work with existing literature is listed in Table IV. The proposed antenna provides good impedance and axial ratio bandwidth when compared to existing antennas, suitable for 5G applications.

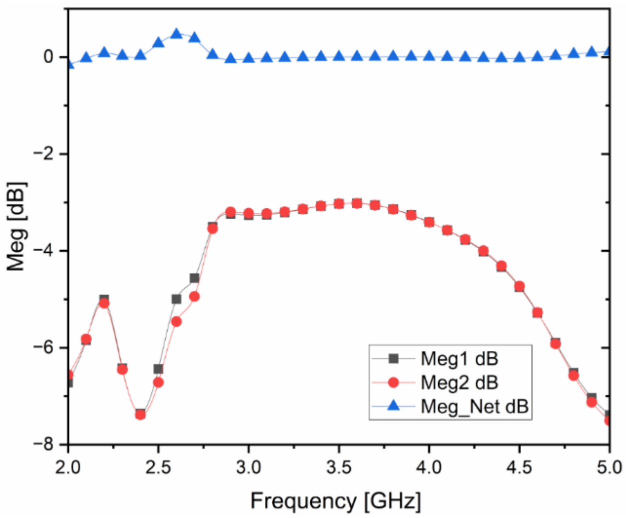

Fig. 16. MEG characteristics of the MIMO antenna.

CONCLUSION

The proposed antenna design is effective in achieving a wide bandwidth for MIMO applications in high-speed 5G networks. The design seems to be very promising as it operates effectively across a wide frequency range and exhibits excellent characteristics. The antennas are configured horizontally with added decoupling for optimum mutual coupling. The system provides a diversity gain beyond 9.98, an ECC below 0.02, and minimal CCL. The TARC and MEG have also been analyzed. Calculation results indicate low channel capacity losses of less than 0.25 bits/sec/Hz, a TARC below −15 dB across the entire frequency band, and the MEG value lies in between the required range, which produces good diversity performance. The simplicity of the design, robust radiation performance, wide bandwidth, effective isolation between antennas, and compact size make this system well-suited for forthcoming 5G applications.

REFERENCES

[1] S. Ahmad et al., "A compact CPW-fed ultra-wideband multi-input-multi-output (MIMO) antenna for wireless communication networks," IEEE Access, vol. 10, pp. 25278–25289, 2022.
[2] S.-W. Kim, G.-S. Kim, and D.-Y. Choi, "CPW-fed wideband circular polarized antenna for UHF RFID applications," Int. J. Antennas Propag., vol. 2017, pp. 1–7, 2017.
[3] P. Tiwari, V. Gahlaut, M. Kaushik, P. Rani, A. Shastri, and B. Singh, "Advancing 5G connectivity: A comprehensive review of MIMO antennas for 5G applications," Int. J. Antennas Propag., vol. 2023, pp. 1–19, 2023.
[4] S. A. Khwandah, J. P. Cosmas, P. I. Lazaridis, Z. D. Zaharis, and I. P. Chochliouros, "Massive MIMO systems for 5G communications," Wirel. Pers. Commun., vol. 120, no. 3, pp. 2101–2115, 2021.
[5] S. Kulkarni, Department of Electronics and Instrumentation, Gulbarga University, Gulbarga (Karnataka), India., D. R. Y. Kulkarni, and Department of Electronics and Communication Engineering, Gulbarga University, Gulbarga (Karnataka), India., "Surveying on MIMO technology for future wireless communication," International Journal of Recent Technology and Engineering (IJRTE), vol. 10, no. 4, pp. 78–83, 2021.
[6] G. Bharti, D. Kumar, A. K. Gautam, and A. Sharma, "Two-port dual-band circularly polarized dielectric resonator-based MIMO antenna with polarization diversity," Electromagnetics, vol. 40, no. 7, pp. 463–478, 2020.
[7] P. Sharma, R. N. Tiwari, P. Singh, P. Kumar, and B. K. Kanaujia, "MIMO antennas: Design approaches, techniques and applications," Sensors (Basel), vol. 22, no. 20, p. 7813, 2022.
[8] V. Kaim, B. K. Kanaujia, S. Kumar, H. C. Choi, K. W. Kim, and K. Rambabu, "Ultra-miniature circularly polarized CPW-fed implantable antenna design and its validation for biotelemetry applications," Sci. Rep., vol. 10, no. 1, 2020.
[9] G. Bharti, D. Kumar, A. K. Gautam, and A. Sharma, "Two-port ring-shaped dielectric resonator-based diversity radiator with dual-band and dual-polarized features," Microw. Opt. Technol. Lett., vol. 62, no. 2, pp. 581–588, 2020.
[10] J. Kulkarni, A. Desai, and C.-Y.-D. Sim, "Two port CPW-fed MIMO antenna with wide bandwidth and high isolation for future wireless applications," Int. J. RF Microw. Comput-Aid. Eng., vol. 31, no. 8, 2021.
[11] D. Lodhi and S. Singhal, "CPW fed shovel shaped super wideband MIMO antenna for 5G applications," Int. J. Electron. Commun., vol. 168, no. 154700, p. 154700, 2023.
[12] C.-Z. Du, K.-J. Li, and S.-S. Zhong, "A novel flexible hexagon wideband CPW-fed monopole antenna for UWB applications," Microw. Opt. Technol. Lett., vol. 63, no. 7, pp. 1899–1905, 2021.
[13] P. Kim-Thi and Tung The-Lam Nguyen, "Circularly polarized MIMO patch antenna with high isolation and wideband characteristics for WLAN applications," Heliyon, vol. 9, no. 9, p. e19450, 2023.
[14] R. Kumar and R. K. Chaudhary, "Circularly polarized rectangular DRA coupled through orthogonal slot excited with microstrip circular ring feeding structure for Wi-MAX applications," Int. J. RF Microw. Comput-Aid. Eng., vol. 28, no. 1, p. e21153, 2018.
[15] N. Hussain, T. Pham, and H.-H. Tran, "Circularly polarized MIMO antenna with wideband and high isolation characteristics for C-band communication systems," Micromachines (Basel), vol. 13, no. 11, p. 1894, 2022.
[16] S. Rajkumar, N. Vivek Sivaraman, S. Murali, and K. T. Selvan, "Heptaband swastik arm antenna for MIMO applications," IET Microw. Antennas Propag., vol. 11, no. 9, pp. 1255–1261, 2017.
[17] A. Chowdhury and P. Ranjan, "A novel circularly polarised, CPW-based MIMO antenna for 5G-wireless communication in sub-6 GHz band," Int. J. Electron. Lett., pp. 1–17, 2023.
[18] S. Kumar, A. S. Dixit, R. R. Malekar, H. D. Raut, and L. K. Shevada, "Fifth generation antennas: A comprehensive review of design and performance enhancement techniques," IEEE Access, vol. 8, pp. 163568–163593, 2020.
[19] T. Raj, R. Mishra, P. Kumar, and A. Kapoor, "Advances in MIMO antenna design for 5G: A comprehensive review," Sensors (Basel), vol. 23, no. 14, p. 6329, 2023.
[20] S. Chakraborty, M. A. Rahman, M. A. Hossain, A. T. Mobashsher, E. Nishiyama, and I.

Toyoda, "Design and performance studies of a MIMO antenna with circular polarization diversity for 5G applications," in 2019 5th International Conference on Advances in Electrical Engineering (ICAEE), 2019.

[21] C. Du and Z. Zhao, "A cpw-fed dual-band Mimo antenna with enhanced isolation for 5g application," Prog. Electromagn. Res. M, vol. 98, pp. 11–20, 2020.

[22] P. Tiwari, V. Gahlaut, M. Kaushik, P. Rani, A. Shastri, and B. Singh, "Advancing 5G connectivity: A comprehensive review of MIMO antennas for 5G applications," Int. J. Antennas Propag., vol. 2023, pp. 1–19, 2023.

[23] K. Du, Y. Wang, and Y. Hu, "Design and analysis on decoupling techniques for MIMO wireless systems in 5G applications," Appl. Sci. (Basel), vol. 12, no. 8, p. 3816, 2022.

[24] A. W. M. Saadh, P. Ramaswamy, and T. Ali, "A CPW fed two and four element antenna with reduced mutual coupling between the antenna elements for wireless applications," Appl. Phys. A Mater. Sci. Process., vol. 127, no. 2, 2021.

[25] J. Iqbal, U. Illahi, M. I. Sulaiman, M. M. Alam, M. M. Suud, and M. N. Mohd Yasin, "Mutual coupling reduction using hybrid technique in wideband circularly polarized MIMO antenna for WiMAX applications," IEEE Access, vol. 7, pp. 40951–40958, 2019.

[26] A. K. Dwivedi, A. Sharma, A. K. Pandey, and V. Singh, "Two port circularly polarized MIMO antenna design and investigation for 5G communication systems," Wirel. Pers. Commun., vol. 120, no. 3, pp. 2085–2099, 2021.

[27] R. Ma, H. Huang, X. Li, and X. Wang, "Triple-band MIMO antenna with integrated decoupling technology," Int. J. Antennas Propag., vol. 2023, pp. 1–14, 2023.

[28] A. Baz, D. Jansari, S. P. Lavadiya, and S. K. Patel, "Miniaturized and high gain circularly slotted 4×4 MIMO antenna with diversity performance analysis for 5G/Wi-Fi/WLAN wireless communication applications," Results Eng., vol. 20, no. 101505, p. 101505, 2023.

[29] G. Bharti, D. Kumar, A. K. Gautam, and A. Sharma, "Two-port ring-shaped dielectric resonator-based diversity radiator with dual-band and dual-polarized features," Microw. Opt. Technol. Lett., vol. 62, no. 2, pp. 581–588, 2020.

[30] D. El Hadri, A. Zugari, A. Zakriti, and M. El Ouahabi, "Dual-band MIMO antenna with four CPW elements using polarization diversity for 5G mobile communication networks and satellite," Adv. Electromagn., vol. 12, no. 3, pp. 43–53, 2023.

